


 Cite this: *RSC Adv.*, 2022, 12, 19246

Array-based chemical warfare agent discrimination via organophosphorus-H₂O₂ reaction-regulated chemiluminescence

 Qiaoli Zhang,^a Yang Yang,^{*a} Junmei Xia,^a Yingying Zhang,^a Shilei Liu^{*a} and Zhiqin Yuan ^{*b}

It has been a challenge to achieve rapid, simple, and effective discrimination of organophosphorus nerve agents (typical chemical warfare agents) due to the similar chemical properties of the targets such as sarin, soman, cyclosarin and VX. In this study, we propose a chemiluminescence sensor array that can effectively discriminate organophosphorus nerve agents by organophosphorus-H₂O₂ reaction, which produces peroxyphosphonate intermediate and regulates the chemiluminescence intensity. A simple chemiluminescence sensor array based on different chemiluminescence characteristics of the four organophosphorus nerve agents in the luminol-H₂O₂ system and layered double hydroxide-luminol-H₂O₂ system has been constructed. Four agents can be well distinguished at a concentration of 1.0 mg L⁻¹ when linear discriminant analyses and hierarchical cluster analyses are smartly combined. The high accuracy (100%) evaluation of 20 blind samples demonstrates the practicability of this proposed chemiluminescence sensor array.

 Received 15th April 2022
 Accepted 17th June 2022

DOI: 10.1039/d2ra02420a

rsc.li/rsc-advances

Introduction

In spite of the validation of Chemical Weapons Convention since 1997, chemical weapons are still in use, especially in armed conflicts. The major components of chemical weapons, also known as chemical warfare agents (CWAs), cause a serious health threat and even death through inhibiting enzymatic activity or destroying organs, and can be primarily divided into two categories, nerve agents and blister agents.^{1–3} Among these CWAs, organophosphorus nerve agents (OPNAs) that disrupt neurological regulation of biological systems by suppressing organophosphorus cholinesterase are more toxic and frequently used.^{4,5} Therefore, the development of simple and sensitive methods for detecting them is essential to prevent humans from WMA threat or terrorist attack. Toward this goal, many analytical methods based on chromatography, mass spectrometry, and spectroscopy have been constructed for the detection of OPNAs or simulants.^{6–17} Nevertheless, the molecular differences between known OPNAs are very tiny. For example, sarin (GB), soman (GD), cyclosarin (GF) and VX only have a small variation in one or two substitution groups.¹⁸ The tiny structural variation, as well as the small chemical reactivity difference, makes the rapid discrimination of them difficult.

Thus, exploring an effective method for differentiating these nerve agents is still appealing.

Array-based sensing methods, also called “chemical nose/tongue” tactics, show great potentials in the differentiation of analytes with similar structures and/or chemical/physical properties.¹⁹ In general, the unique patterns from analyte-sensing elements interactions are quantized through linear discriminant analysis (LDA) technique.²⁰ In this case, the utilization of selective rather than specific interaction enables the successful discrimination of different targets, such as proteins, cells, isomers and analogues.^{21–25} Thus, the exploration of an array-based sensing method for discriminating organophosphorus-based nerve agents is inspired. Chemiluminescence (CL) spectrophotometry with free light source and ultralow background has been extensively used in the design of rapid response detection systems.^{26–30} Hence, it is encouraged to propose a rapid and effective CL sensor array for the differentiation of various nerve agents, which is theoretically possible.

In this work, we speculate that proper CL systems with response to OPNAs can be applied in constructing CWA sensor array. The organophosphorus compounds are reported to react with hydrogen peroxide (H₂O₂) and form peroxyphosphonate (PPA) intermediate.^{31–33} It can be described that the formed PPA can react with luminol, which enhances the CL intensity. On the other hand, the hydrolysis of PPA generates pinacolyl methylphosphate (PMPA), which competes with the subsequent CL reaction and diminishes the CL signal, as shown in Fig. 1. As a result, the CL responses toward various PPAs from

^aState Key Laboratory of NBC Protection for Civilian, Beijing 102205, China. E-mail: ricdyihui@163.com; liu_shilei@lacrictd.com

^bState Key Laboratory of Chemical Resource Engineering, College of Chemistry, Beijing University of Chemical Technology, Beijing 100029, China. E-mail: yuanzq@mail.buct.edu.cn



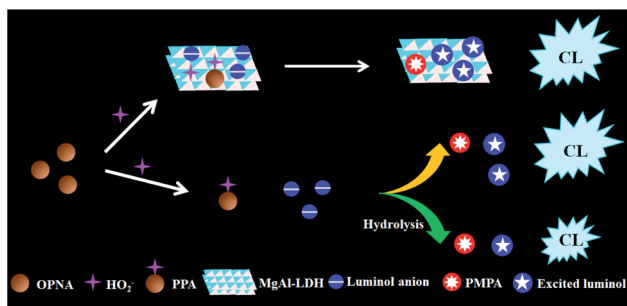


Fig. 1 Schematic illustration of organophosphorus nerve agent-induced change of CL signal.

corresponding OPNAs are theoretically different. Herein, we described our attempts to apply luminol–H₂O₂ related CL systems into array-based OPNAs discrimination. As a case study, luminol–H₂O₂ and layered double hydroxide (MgAl-LDH)–luminol–H₂O₂ systems are used for the development of OPNAs sensor array. The detection mechanism is based on the unique CL response patterns generated from two CL systems and quantification analysis with LDA technique. To our knowledge, this is the first example of high-throughput OPNAs discrimination without any combination of pretreatment technique. The practical application of the proposed chemiluminescence sensor array was further verified by the examination of 20 blind samples of single OPNA.

Experimental section

Chemicals and materials

Luminol and sodium hydroxide (NaOH) were purchased from Shanghai Aladdin company (Shanghai, China). Hydrogen peroxide (H₂O₂) were obtained from Tianjin Fengchuan Chemical Reagent Co., Ltd. (Tianjin, China). Mg(NO₃)₂·6H₂O and Al(NO₃)₃·9H₂O were obtained from Sigma-Aldrich Corporation (Shanghai, China). Sodium carbonate (Na₂CO₃) and terephthalic acid (TA) were acquired Beijing Chemical Reagent Company (Beijing, China). Soman (GD), sarin (GB), cyclosarin (GF) and VX were supplied by State Key Laboratory of NBC Protection for Civilian (Beijing, China). All reagents were analytical grade and used without further purification. Deionized water was purchased from A.S. Watson Group Ltd. (Beijing, China). Deionized water used in experiment was purchased from A.S. Watson Group Ltd. (Beijing, China). A 0.03 M stock solution of luminol was prepared by dissolving luminol in 0.1 M NaOH and was used after about 2 weeks in order to make the luminol solution stable. Working solutions of H₂O₂ was prepared daily from 30% H₂O₂.

Synthesis of MgAl-LDH

The MgAl-LDH was synthesized by coprecipitation methods according to previous procedure.^{34,35} The precipitation process was carried out under low supersaturation conditions at constant pH. For Mg/Al molar ratio of 2, solution A was consisted of 0.045 mol Mg(NO₃)₂ and 0.015 mol Al(NO₃)₃ dissolved

in 60 mL deionized water. Solution B was consisted of 0.108 mol NaOH and 0.0075 mol Na₂CO₃ also by dissolving in 60 mL deionized water. The two solutions were added slowly into a 250 mL round bottomed flask under vigorous stirring maintaining pH 10 at room temperature. The resulting white slurry was aged for 24 h at 60 °C. Afterward, the precipitate was collected by centrifugation and washed thoroughly with deionized water for three times, and then the colloidal suspension was diluted to the original concentration and stored for the further use.

Characterization

The chemiluminescence signal was measured on an MPI-EII full spectrum electrochemiluminescence analyzer. (Xi'an Remex Analysis Instruments Co., Ltd, Xi an, China). Chemiluminescence spectra were obtained using an F97pro fluorescence spectrophotometer with a scanning rate of 3000 nm min⁻¹ at 10 nm emission slit, without light source (Lengguang Technology, Shanghai, China). Transmission electron microscopy (TEM) images were collected with a HT7700 transmission electron microscope (Hitachi, Japan). Phosphorus nuclear magnetic resonance (³¹P NMR) spectra were performed with a Bruker Avance III HD 600 NMR spectrometer (Bruker, Switzerland).

CL measurement of OPNA-response of luminol–H₂O₂ system

A static-injection CL setup was conducted in all CL experiments. Briefly, 200 μL luminol (20 μM) was added into a quartz cuvette of chemiluminescence (CL) analyser, then, this quartz cuvette was placed in the cuvette holder. Under complete protection from light, the mixture of 100 μL H₂O₂ (10 mM) and 100 μL GD (1.0 ppm) were stirred about 10 s in centrifuge tube and injected into the above vial using microliter syringes. The chemiluminescence spectra were recorded with the Xenon lamp off. The data integration time of the CL analyzer was set at 1 s per spectrum, and the operating voltage of 800 V was used for the CL detection. CL signals of GB, GF, and VX were measured using the same procedure.

CL measurement of OPNA-response of MgAl-LDH–luminol–H₂O₂ system

The CL measurement procedure is almost same as that of luminol–H₂O₂ system. Firstly, 200 μL luminol (20 μM) and 100 μL MgAl-LDH (10 mg mL⁻¹) solution were added to the sample pool in turn, 100 μL H₂O₂ (10 mM) and 100 μL GD (1.0 ppm) were mixed and injected into the pool. GB, GF and VX were measured using the same procedure.

CL emission spectra measurement

CL emission spectra were measured with a fluorescence spectrophotometer without excitation. To ensure the strong CL intensity, high concentrations of reactants were used. Briefly, 200 μL luminol (50 μM) was added into a quartz cuvette under dark condition. Then, a mixture of 100 μL H₂O₂ (10 mM) and 100 μL acetonitrile or 100 μL GD (1.0 ppm) was injected into the



vial using microliter syringes. GB, GF and VX were measured using the same procedure. The operating voltage of fluorescence spectrophotometer was set to 800 V.

Results and discussion

Mechanism of OPNA-regulated CL

At the starting point, the MgAl-LDH was synthesized according to our reported works with slight modification. The prepared MgAl-LDHs were uniform and close to 50 nm (Fig. 2A). As shown in Fig. 2B, LDHs exhibited sharp and symmetric reflections for (003), (006), (110) and (113) planes with broad and asymmetric reflections for (012), (015) and (018) planes. The baseline is low and stable, indicating that MgAl-LDHs possess

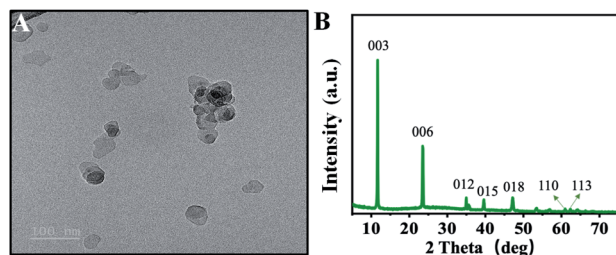


Fig. 2 TEM image (A) and XRD (B) of as-synthesized MgAl-LDH. Scale bar = 100 nm.

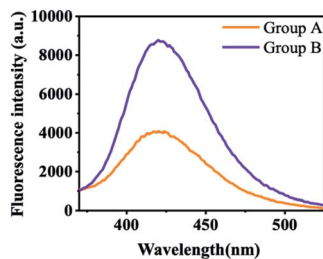


Fig. 3 The fluorescence emission spectra of TA-H₂O₂ solution without (group A) and with (group B) addition of after reaction with MgAl-LDH.

good crystal shape and high regularity between layers. As referred in previous work, the CL intensity of luminol-H₂O₂ system can be boosted by MgAl-LDHs, because the MgAl-LDH possesses horseradish peroxidase-like catalytic activity and benefits the generation of $\cdot\text{OH}$.³⁵ To confirm this assumption, TA was introduced to illustrate the generation of $\cdot\text{OH}$, because TA can react with $\cdot\text{OH}$ and produce fluorescent product hydroxy terephthalic acid (HOTA, $\lambda_{\text{ex}} = 315 \text{ nm}$, $\lambda_{\text{em}} = 425 \text{ nm}$). As shown in Fig. 3, the fluorescence emission of TA-H₂O₂ solution was observed around 425 nm, indicating the formation of HOTA. Interestingly, the fluorescence intensity was largely enhanced after addition of MgAl-LDH. In this case, the introduction of MgAl-LDH can promote the decomposition of H₂O₂ and generation of $\cdot\text{OH}$. In order to verify the CL enhancement, CL signals of luminol-H₂O₂ system were acquired without and with the introduction of MgAl-LDHs. As shown in Fig. 4A, the CL intensity showed visible increment upon adding MgAl-LDHs, which is consistent with our previous results.³⁵ To understand whether the introduction of OPNAs could alter the CL intensity of these systems, the CL signals of luminol-H₂O₂ system and MgAl-LDH-luminol-H₂O₂ system without and with the addition of GD were firstly examined. As manifested in Fig. 4A, the CL signal of luminol-H₂O₂ system upon adding GD was ~ 0.6 folds to the control, indicating the negative effect of GD-improved CL intensity. In addition, the CL signal of MgAl-LDH-luminol-H₂O₂ system was enhanced upon adding GD, indicating the feasibility of organophosphorus nerve agent analysis with luminol-H₂O₂ and MgAl-LDH-luminol-H₂O₂ systems. According to previous reports, the change of CL emission might be attributed to the formation of PPA.³¹ It should be noticed that the peroxide phosphonate in PPA is very active and easily decomposes in basic peroxide.³³ In addition, PPA decomposes quickly under high temperature. As a result, the mass spectra of PPA can't be obtained due to the ultrahigh temperature ($>300 \text{ }^\circ\text{C}$) of ionization source.

It has been reported NMR spectra can achieve CWA analysis with proper derivatization reagent.³⁶ To reveal the mechanism of GD-reduced CL intensity, ³¹P NMR spectra and CL emission spectra were investigated. It was clearly seen that GD with chemical shift of 31.28, 31.91, 35.61 and 36.17 ppm were

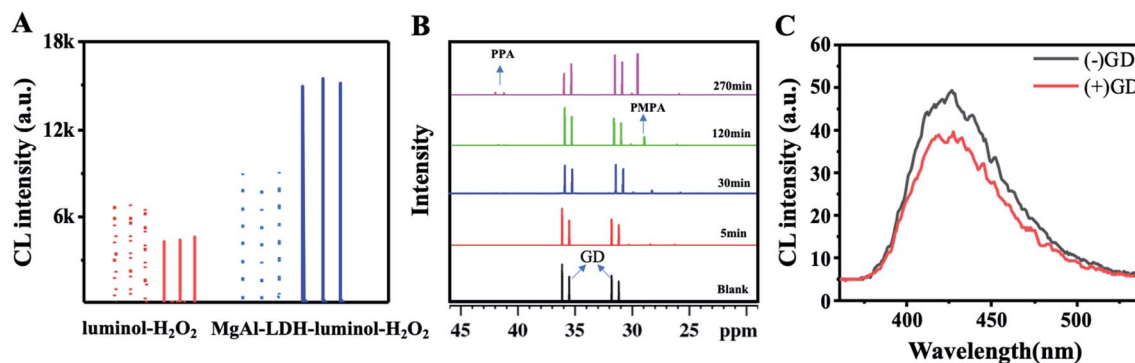


Fig. 4 (A) CL signals of luminol-H₂O₂ (red line) and MgAl-LDH-luminol-H₂O₂ (blue line) systems in absence (dashed line) and presence (solid line) of 1.0 ppm GD. (B) Time-dependent ³¹P NMR spectra of GD upon adding H₂O₂. (C) CL emission spectra of luminol-H₂O₂ system without (black line) and with (red line) the addition of GD.



observed (Fig. 4B), which is consistent with the previous reports.³¹ After the mixture of GD and H₂O₂, two new peaks around 41.97 and 41.31 ppm (two diastereomers) and belong to PPA appeared during reaction, indicating the production of PPA after the mixing of OPNAs and H₂O₂. Accordingly, the signal around 31.28, 31.91, 35.61 and 36.17 ppm decreased upon the reaction, suggesting the continuous consumption of GD. We also found that peaks with chemical shift of 29.31 ppm increased as the increasing reaction time. This peak was assigned to phosphorus of PMPA. Taken together, the reaction between OPNAs and H₂O₂ generates both PPA and PMPA and alters the CL signal.

In addition to reaction kinetics, the CL signals are also affected by the emissive species. To further understand whether new emissive species is produced upon introducing GD, the CL emission spectra of luminol–H₂O₂ system in the absence and presence of GD were also measured. As shown in Fig. 4C, the emission maximum of luminol–H₂O₂ system was located around 425 nm, which is assigned for the excited luminol radical. However, the addition of GD didn't cause any variation in CL emission spectral shape except varied CL intensity, ruling out the formation of any new emissive product. Taken these data together, we can confirm that the GD-mediated CL intensity is due to the formation of GD-corresponding PPA, which inhibits the generation of excited luminol radical. Taken together, these results suggest the feasibility of OPNA-regulated CL signal of luminol–H₂O₂ system by forming PPA and PMPA. Since OPNAs have similar structure, we proposed that OPNAs might change the CL with the same mechanism, and the schematic illustration was displayed in Fig. 1.

Optimize of luminol–H₂O₂/MgAl-LDH–luminol–H₂O₂ sensing platform

The GD-induced CL signal variation in both luminol–H₂O₂ and MgAl-LDH–luminol–H₂O₂ systems suggests the possibility of the exploration of OPNA sensor array based on these two systems. Before the conduction of sensor array, the optimization of luminol, H₂O₂ and MgAl-LDH concentrations upon the addition of 1.0 ppm GD was conducted. According to Fig. 5A, the CL intensity increment showed an increment with the increased luminol concentration from 10 to 20 μM, and

decreased with further increased luminol. This might be attributed the limited formation of PPA, which only oxidizes certain luminol. Thus, further increasing luminol has no enhancement of CL. The relative CL intensity increment also gradually enhanced with the increasing H₂O₂ concentration from 5 to 10 mM (Fig. 5B). However, it decreased with further increasing H₂O₂ concentration. As indicated in our previous reported,³⁴ the MgAl-LDH concentration plays an important role on the CL intensity to luminol–H₂O₂ system, thus it might also affect the CL increment in this work. As shown in Fig. 5C, maximum relative CL increment was found when the MgAl-LDH concentration was 10 mg mL⁻¹. The large specific area and positively charged layer of MgAl-LDH facilitate the approaching of H₂O₂/PPA and luminol anion through adsorption interaction.³⁴ However, high MgAl-LDH concentration may reduce the local concentration of reactants, and then weakens the CL. To achieve sensitive detection, the concentrations of H₂O₂, MgAl-LDH and luminol at 20 μM, 10 mM, and 10 mg mL⁻¹ were chosen in following experiments.

CL sensor array-based OPNA discrimination

In spite of the small structural differences of four OPNAs (Fig. 6A), their reactivity might be different. We first calculated the molecular electronegativity of phosphorus element in four OPNAs by Gaussview software. The charge distribution of phosphorus in GD (1.341) was higher than that of VX (1.026). And middle phosphorus electronegativities were obtained in GB (1.329) and GF (1.328). These results indicate that GD might possess higher reactivity toward H₂O₂ in comparison to GB, GF, and VX. As referred above, certain GD caused CL variations of both systems, and MgAl-LDH involvement would affect the reactant interaction and generate apparent CL profiles. Then, we tried to use the two CL systems to construct the sensor array. The primary advantage of array-based detection is no need of differentiation of drivers, and the analyte-sensing element interactions are understood mechanically. To ensure that we were able to detect and distinguish four OPNAs, we chose 1.0 ppm OPNAs to create the CL response pattern. That is, for each OPNA, we recorded its CL response against two CL systems for five repeats, producing a 2 × 4 × 5 matrix (Fig. 6B). The CL increment was only observed upon adding VX in luminol–H₂O₂

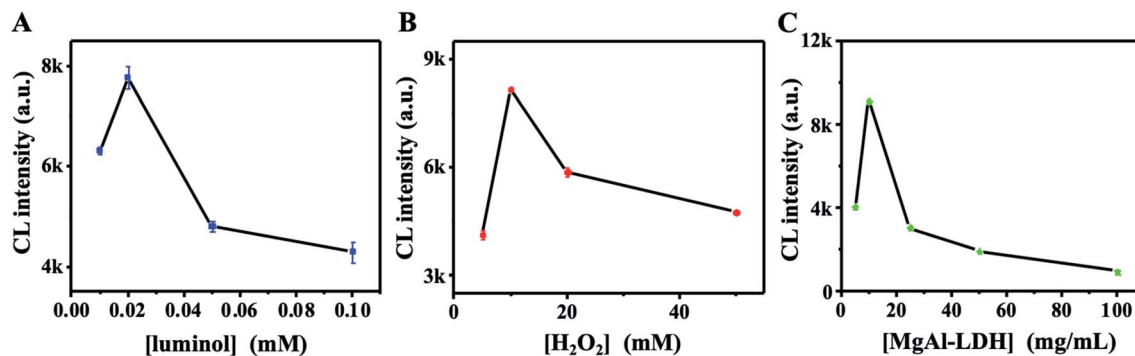


Fig. 5 Optimization of CL reaction. CL intensity plots of luminol–H₂O₂ system with various concentrations of luminol (A), H₂O₂ (B) and MgAl-LDH (C) in the presence of 1.0 ppm GD.

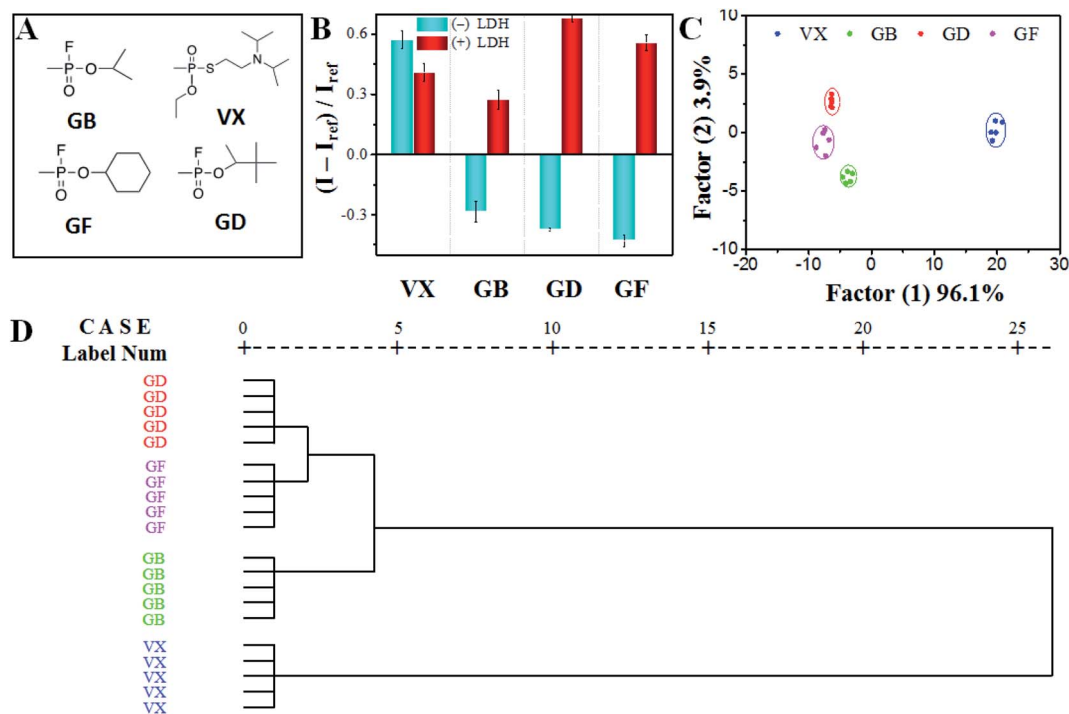


Fig. 6 Discrimination of four OPNAs with CL sensor array. (A) Molecular structures of four OPNAs. (B) Relative CL intensity increment $(I - I_{ref})/I_{ref}$ patterns of the sensor array against four OPNAs as an average of five parallel measurements. (C) Canonical score plots for the first two factors of relative fluorescence increase $(I - I_{ref})/I_{ref}$ pattern from four OPNAs analyzed by LDA. (D) HCA analysis of OPNA samples with five parallel measurements.

system, while GB, GD and GF caused CL decrement. Such a phenomenon might be attributed to the different stabilities of corresponding PPAs. As referred in previous work, PPA from VX shows higher stability in comparison with other PPAs.³¹ In this case, the oxidation of luminol can be promoted and the CL intensity is enhanced by VX. And the hydrolysis of other three PPAs inhibits the oxidation of luminol and produces weak CL signal. On the other hand, all of these OPNAs induced visible CL enhancement in MgAl-LDH-luminol- H_2O_2 system. A possible responsible reason is that large specific area and positively charged layer of MgAl-LDH facilitate the adsorption of peroxide anion and luminol anion. The formed PPAs on MgAl-LDH easily react with adjacent luminol anion and produce excited luminol radical. As a result, the CL intensity is boosted. The dramatic difference on relative CL increment patterns $(I - I_0)/I_0$ induced by four OPNAs indicates the feasibility of OPNAs discrimination using this sensor array because of the generally unique response pattern of each OPNA generated by sensor array.

To further realize the differentiation of four OPNAs, the raw data of generated CL response patterns were subjected to LDA using SPSS software version 19.0. It was seen in Fig. 6C, the resulted canonical patterns were visualized as a two-dimensional score plot with excellent clustering and satisfied dispersion with 100% of the total variance, indicating the powerful discrimination of four OPNAs with proposed sensor array. In addition, hierarchical cluster analysis (HCA) was used to determine the similarity of OPNAs through the Euclidean distance-based statistical classification. Interestingly, all 20 cases (4 OPNAs \times 5 replicates) were correctly assigned to their

respective groups, as shown in Fig. 6D, further demonstrating the capability of the designed sensor array for OPNAs differentiation. In a word, the characteristic and highly reproducible CL response patterns induced by particular OPNA confirm the

Table 1 Identification of 20 unknown sole OPNA samples

| # | $(I - I_{ref})/I_{ref}$ | | Identi. | Verifi. |
|----|-------------------------|--------------|---------|---------|
| | (-) MgAl-LDH | (+) MgAl-LDH | | |
| 1 | 0.612 | 0.385 | VX | VX |
| 2 | 0.574 | 0.478 | VX | VX |
| 3 | -0.369 | 0.236 | GB | GB |
| 4 | -0.356 | 0.682 | GD | GD |
| 5 | -0.373 | 0.650 | GD | GD |
| 6 | -0.343 | 0.236 | GB | GB |
| 7 | -0.262 | 0.285 | GB | GB |
| 8 | -0.379 | 0.723 | GD | GD |
| 9 | -0.379 | 0.699 | GD | GD |
| 10 | -0.456 | 0.442 | GF | GF |
| 11 | -0.457 | 0.745 | GF | GF |
| 12 | 0.582 | 0.391 | VX | VX |
| 13 | -0.243 | 0.228 | GB | GB |
| 14 | -0.380 | 0.656 | GD | GD |
| 15 | -0.435 | 0.644 | GF | GF |
| 16 | 0.537 | 0.399 | VX | VX |
| 17 | -0.232 | 0.271 | GB | GB |
| 18 | -0.408 | 0.533 | GF | GF |
| 19 | 0.605 | 0.451 | VX | VX |
| 20 | -0.397 | 0.389 | GF | GF |



Table 2 Comparison of this work with different methods detection nerve agents and mimics^a

| # | Target | Strategy | LOD (ng L ⁻¹) | Multiple analytes | Ref. |
|----|--------------------|-----------------------------|---|-------------------|------------|
| 1 | DCP(l) | Fluorimetry | 3.40 | No | 37 |
| 2 | DCP(l) | Fluorimetry | 5.20 × 10 ² | No | 38 |
| 3 | DCP(g) | Fluorimetry | 12.42 | No | 39 |
| 4 | DCP(g) | Fluorimetry | 0.15 | No | 40 |
| 5 | DCP(g) | Fluorimetry and colorimetry | 1.70 × 10 ² | No | 41 |
| 6 | DCP(g); GB(g) | Fluorimetry | 4.40; 7.00 | No | 42 |
| 7 | DMMP(g) | Liquid array | 2.00 | No | 43 |
| 8 | DCP(l); DCNP(l) | Colorimetry | 6.03 × 10 ² ; 5.87 × 10 ³ | Yes | 44 |
| 9 | DCP(l); DFP(l) | Fluorimetry | 2.59; 6.4 | Yes | 45 |
| 10 | GD(l); DCP(l) | Fluorimetry and colorimetry | 6.12 × 10 ² ; 5.79 × 10 ² | Yes | 46 |
| 11 | DCP(g); CEES(g) | Fluorimetry | 8.00; 3.00 × 10 ² | No | 47 |
| 2 | GB; GD; GA; VX (l) | Fluorimetry | 7.00 × 10 ⁵ ; 9.10 × 10 ⁵ ; 8.10 × 10 ⁵ ; 1.34 × 10 ⁶ | Yes | 48 |
| 13 | GB; GD; GF; VX (l) | CL sensor array | 1.0 × 10 ³ | Yes | This study |

^a (g) gas phase, (l) solution.

excellent reproducibility of OPNA identification using the proposed sensor array.

The CL sensor array by luminol–H₂O₂ and MgAl-LDH–luminol/H₂O₂ systems can be chosen working array for OPNA differentiation due to the advantages of good identification and reproducibility. To verify the detection accuracy of the OPNA sensor array, a series of OPNA solutions (final concentration of 1.0 ppm) were chosen as the blind samples. Conformably, the CL response patterns were acquired with the same approach and subjected to LDA analysis. Notably, as displayed in Table 1, of the 20 blind OPNA samples, none of them was incorrectly identified, accordingly providing an identification accuracy of 100%. The favourable identification accuracy further validated that this proposed CL sensor array exhibits a convincing ability for OPNA discrimination with high efficiency (Table 2).^{37–48} The sensor array strategy requires selective but not specific interaction, and thus the achievement of chemical reactivity-based target discrimination is also possible. Therefore, the combination of the “chemical nose/tongue” strategy with specific chemical reaction may facilitate analysis of other similar analytes and/or analogues with tiny difference.

Conclusions

In conclusion, we have successfully achieved the spectrophotometric discrimination of four OPNAs based on luminol–H₂O₂/MgAl-LDH–luminol–H₂O₂ CL sensor array by utilizing organophosphorus–H₂O₂ reaction. With the incorporation of LDA-based mechanical understanding, this system identifies CWAs without use of any separation technique. Additionally, the practical application of this sensor array is firmly validated by the high accuracy of 20 blind sample tests. Moreover, such an effective CWA sensor array may also have the prospect for selective CWA antidotes discovery. Our work not only present a CL sensor array for differentiating CWAs, but also provide a possible tactic for designing versatile sensor array by involving specific chemical reactions. Thus, new avenues for the development of simple and sensitive protocols for the differentiation

of targets (e.g., pesticides, weedicides and drugs) with tiny structural difference and chemical reactivity without separation based on a similar tactic are now possible in environmental, analytical chemistry and life science-related fields.

Conflicts of interest

There are no conflicts to declare.

Acknowledgements

This work was supported by the National Natural Science Foundation of China (22074005), the Natural Science Foundation of Beijing Municipality (2202038).

Notes and references

- M. Schwenk, *Toxicol. Lett.*, 2018, **293**, 253–263.
- D. H. Blakey, M. Lafontaine, J. Lavigne, D. Sokolowski, J.-M. Philippe, J.-M. Saponi, W. Biederbick, R. Horre, W. B. Marzi, H. Kondo, Y. Kuroki, A. Namera, T. Okumura, M. Yamamoto, M. Yashiki, P. G. Blain, D. R. Russell, S. M. Cibulsky and D. A. Jett, *BMC Publ. Health*, 2013, **13**, 253.
- H. Niemikoski, K. K. Lehtonen, A. Ahvo, I. Heiskanen and P. Vanninen, *Aquat. Toxicol.*, 2021, **241**, 105993.
- X. Lu, Z. Zhang, R. Gao, H. Wang and J. Xiao, *Forensic Toxicol.*, 2021, **39**, 334–349.
- A. Delaune, S. Mansour, B. Picard, P. Carrasqueira, I. Chataigner, L. Jean, P.-Y. Renard, J.-C. M. Monbaliu and J. Legros, *Green Chem.*, 2021, **23**, 2925–2930.
- J. Puton and J. Namieśnik, *TrAC, Trends Anal. Chem.*, 2016, **85**, 10–20.
- Z. Witkiewicz and S. Neffe, *TrAC, Trends Anal. Chem.*, 2020, **130**, 115960.
- M. R. Sambrook and S. Notman, *Chem. Soc. Rev.*, 2013, **42**, 9251–9267.
- S. Fan, G. Zhang, G. H. Dennison, N. FitzGerald, P. L. Burn, I. R. Gentle and P. E. Shaw, *Adv. Mater.*, 2020, **32**, 1905785.



- 10 G. Liu and Y. Lin, *Anal. Chem.*, 2005, **77**, 5894–5901.
- 11 V. Kumar, *Chem. Commun.*, 2021, **57**, 3430–3444.
- 12 H.-H. Bai, L. Guo, J.-L. Feng, F. Cui-Ling, J. Chen and J.-W. Xie, *Chin. J. Anal. Chem.*, 2008, **36**, 1269–1272.
- 13 W.-h. Wu, J.-j. Dong, X. Wang, J. Li, S.-h. Sui, G.-y. Chen, J.-w. Liu and M. Zhang, *Analyst*, 2012, **137**, 3224–3226.
- 14 H. Xu, H. Zhang, L. Zhao, C. Peng, G. Liu and T. Cheng, *New J. Chem.*, 2020, **44**, 10713–10718.
- 15 C. Zhou, S. Zhang, H. Pan, G. Yang, L. Wang, C.-a. Tao and H. Li, *RSC Adv.*, 2021, **11**, 22125–22130.
- 16 S. Zhang, C. Zhou, B. Yang, Y. Zhao, L. Wang, B. Yuan and H. Li, *New J. Chem.*, 2021, **45**, 7564–7570.
- 17 N. Tuccitto, G. Catania, A. Pappalardo and G. Trusso Sfrazzetto, *Chem.–Eur. J.*, 2021, **27**, 13715–13718.
- 18 K. Kim, O. G. Tsay, D. A. Atwood and D. G. Churchill, *Chem. Rev.*, 2011, **111**, 5345–5403.
- 19 Z. Li, J. R. Askim and K. S. Suslick, *Chem. Rev.*, 2019, **119**, 231–292.
- 20 W. He, L. Luo, Q. Liu and Z. Chen, *Anal. Chem.*, 2018, **90**, 4770–4775.
- 21 N. D. B. Le, G. Yesilbag Tonga, R. Mout, S.-T. Kim, M. E. Wille, S. Rana, K. A. Dunphy, D. J. Jerry, M. Yazdani, R. Ramanathan, C. M. Rotello and V. M. Rotello, *J. Am. Chem. Soc.*, 2017, **139**, 8008–8012.
- 22 H. Yang, F. Lu, Y. Sun, Z. Yuan and C. Lu, *Anal. Chem.*, 2018, **90**, 12846–12853.
- 23 Z. Yuan, Y. Du, Y.-T. Tseng, M. Peng, N. Cai, Y. He, H.-T. Chang and E. S. Yeung, *Anal. Chem.*, 2015, **87**, 4253–4259.
- 24 Y. Sun, F. Lu, H. Yang, C. Ding, Z. Yuan and C. Lu, *Nanoscale*, 2019, **11**, 12889–12897.
- 25 J. Han, H. Cheng, B. Wang, M. S. Braun, X. Fan, M. Bender, W. Huang, C. Domhan, W. Mier, T. Lindner, K. Sehafer, M. Wink and U. H. F. Bunz, *Angew. Chem., Int. Ed.*, 2017, **56**, 15246–15251.
- 26 Z. Li, D. Wang, Z. Yuan and C. Lu, *Anal. Bioanal. Chem.*, 2016, **408**, 8779–8786.
- 27 J. Lou, X. Tang, H. Zhang, W. Guan and C. Lu, *Angew. Chem., Int. Ed.*, 2021, **60**, 13029–13034.
- 28 Y. Yan, X.-y. Wang, X. Hai, W. Song, C. Ding, J. Cao and S. Bi, *TrAC, Trends Anal. Chem.*, 2020, **123**, 115755.
- 29 Y. Chen, Z. Chen, L. Fang, A. Weng, F. Luo, L. Guo, B. Qiu and Z. Lin, *J. Anal. Test.*, 2020, **4**, 128–135.
- 30 T. H. Fereja, F. Du, C. Wang, D. Snizhko, Y. Guan and G. Xu, *J. Anal. Test.*, 2020, **4**, 76–91.
- 31 G. W. Wagner and Y.-C. Yang, *Ind. Eng. Chem. Res.*, 2002, **41**, 1925–1928.
- 32 L. Larsson, B. Wickberg, E. Stenhagen, L. G. Sillén, B. Zaar and E. Diczfalusy, *Acta Chem. Scand.*, 1958, **12**, 723–730.
- 33 J. Epstein, M. Demek and D. Rosenblatt, *J. Org. Chem.*, 1956, **21**, 796–797.
- 34 F. Pan, Y. Zhang, Z. Yuan and C. Lu, *ACS Omega*, 2018, **3**, 18836–18842.
- 35 Z. Wang, F. Liu and C. Lu, *Chem. Commun.*, 2011, **47**, 5479–5481.
- 36 G.-L. Huang, L. Yuan, S.-L. Liu and S.-K. Zhou, *Chin. J. Anal. Chem.*, 2015, **43**, 1927–1933.
- 37 X. Huang, Z. Jiao, Z. Guo, J. Yang, P. Alam, Y. Liu, Y. Men, P. Zhang, H. Feng, S. Yao and B. Tang, *ACS Mater. Lett.*, 2021, **3**, 249–254.
- 38 S. Jindal, V. Maka, G. Anjum and J. Moorthy, *ACS Appl. Mater.*, 2021, **4**, 449–458.
- 39 L. Zeng, H. Zeng, L. Jiang, S. Wang, J.-T. Hou and J. Yoon, *Anal. Chem.*, 2019, **91**, 12070–12076.
- 40 X. Li, Y. Lv, S. Chang, H. Liu, W. Mo, H. Ma, C. Zhou, S. Zhang and B. Yang, *Anal. Chem.*, 2019, **91**, 10927–10931.
- 41 W. Xuan, Y. Cao, J. Zhou and W. Wang, *Chem. Commun.*, 2013, **49**, 10474–10476.
- 42 X. Feng, Y. Wang, W. Feng and Y. Peng, *Chin. Chem. Lett.*, 2020, **31**, 2960–2964.
- 43 J. Liu, T. Wang, J. Xiao and L. Yu, *Microchem. J.*, 2022, **178**, 107334.
- 44 J. Zhao, M. Qing and J. You, *Dyes Pigments*, 2022, **197**, 109870.
- 45 F. Dgnaw, Y. Cai and Q. Song, *Dyes Pigments*, 2021, **189**, 109257.
- 46 Y. Kim, Y. Jang, D. Lee and B.-S. Kim, *Sens. Actuators, B*, 2017, **238**, 145–147.
- 47 W. Xiong, Y. Gong, Y. Che and J. Zhao, *Anal. Chem.*, 2019, **91**, 1711–1714.
- 48 B. Diaz de Grenu, D. Moreno, T. Torroba, A. Berg, J. Gunnars, T. Nilsson, R. Nyman, M. Persson, I. Eklind and P. Wasterby, *J. Am. Chem. Soc.*, 2014, **136**, 4125–4128.

